Transactions, **SMiRT-26**
Berlin/Potsdam, Germany, July 10-15, 2022
Division III

CHARACTERISTICS OF AN ULTRA-HIGH-PERFORMANCE-CONCRETE (UHPC) AGAINST IMPACT LOADING PART 1: BASIC CHARACTERISTICS TEST AND EVALUATION OF BEARING FORCE OF UHPCS

Kenzo Kodera[1], Kyosuke Kamito[2], Kensuke Morita[3], Ritsu Hagiwara[4],

Hideyoshi Watanabe[5], and Shinichi Takezaki[6]

[1] Member, Taisei Corporation, Tokyo, Japan (kdrknz00@pub.taisei.co.jp)
[2] Senior Engineer, Mitsubishi Heavy Industries, Ltd., Hyogo, Japan
[3] Unit Leader, Hitachi-GE Nuclear Energy, Ltd., Ibaraki, Japan
[4] Deputy Manager, Toshiba Energy Systems & Solutions Corporation, Kanagawa, Japan
[5] Chief Research Engineer, Taisei Corporation, Tokyo, Japan
[6] Senior Research Engineer, Taisei Corporation, Tokyo, Japan

ABSTRACT

In the design of nuclear power plants, ensuring the impact resistance of buildings against external hazards, such as tornado missiles and aircraft impact (APC), is necessary. When normal-strength concrete is used to improve the impact resistance of buildings, there is an issue with the member thickness being thicker against external hazards, especially APC. Ultra-high-performance concretes (UHPCs) are considered effective in improving the safety of buildings and reducing the member thickness; however, a proper understanding of the ultimate strength and performance of UHPCs against impact loading is lacking. Therefore, in this study, the ultimate strength of UHPCs against impact loading was evaluated through experiments. The results indicated that the UHPCs had better impact resistance than that of conventional normal-strength concrete, and it was confirmed that the performance of UHPCs could be evaluated using finite element method analysis and the existing formula.

INTRODUCTION

This study had been carried out in the project "Development of technical infrastructure for upgrading materials, structures and construction methods of nuclear power plant buildings". This project aimed to investigate the feasibility of applying ultra-high-performance concretes (UHPCs) to nuclear power plants (NPPs) for improving the resistance of NPP buildings against impact loading. This paper is divided into three parts (outline is shown in Figure 1). Part 1 presents the experimental results of the basic characteristics related to the global failure of the structural walls using UHPCs. Part 2 presents the basic characteristics of UHPCs against impact loading through experiments. Part 3 presents the results of the preliminary analysis conducted to investigate the feasibility of NPPs using UHPCs against impact loading, based on the results of parts 1 and 2.

According to Nuclear Energy Institution (2011), for NPP buildings to achieve impact resistance, it is crucial to design structural walls that can: (1) prevent local failures, such as perforation and scabbing of the back surface by missiles; and (2) prevent global failure under impact loading. The design for the prevention of global failure requires the evaluation of the bending performance and punching shear strength of the structural members, while that for the prevention of local failure requires perforation and scabbing assessment. For reinforced concretes (RCs) using normal-strength concrete, the structural walls of buildings could be massive against severe impact loading. Therefore, it is conceivable to reduce the member thickness using UHPCs, which are expected to improve the impact resistance. UHPCs are ultra-high-strength fiber-reinforced concretes. However, the impact resistance performance of UHPCs has not been fully clarified. Therefore, bending and punching shear tests were conducted to understand the basic characteristics related to the global failure of the structural members using UHPCs.

In this study, two types of UHPCs were selected: Fc150 (150-MPa ultra-high-performance steel-fiber-reinforced concrete containing polypropylene fiber) and UFC (180-MPa ultra-high-performance steel-fiber-reinforced concrete). Fc150 contains 0.11 vol% (1 kg/m^3) polypropylene fiber and 1.0 vol% (78.5 kg/m^3) steel fiber, while UFC contains 2.0 vol% (157 kg/m^3) steel fiber. Fc150 contains coarse aggregate whereas UFC does not. UFC was adopted as part of a composite member (wall or roof) with Fc33, to conduct the tests. In the composite member, UFC was applied to the collision surface side (concrete compression side), and Fc33 was applied to the collision back surface side. Hereinafter, this composite member is called UFC+Fc33. In addition to the UHPCs, Fc33 (33-N/mm^2 normal-strength concrete) was tested for comparison in this study.

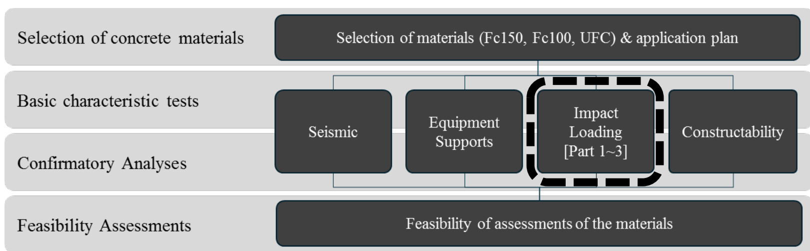

Figure 1. Outline of this project

STUDY OF BENDING PERFORMANCE

For RC members using UHPC and those using normal concrete protected by UFC panels, the static bending tests of the beams were conducted to investigate the bending characteristics related to global failure in aircraft impact (APC). The ultimate material strain was evaluated using the experimental results and simulation analysis.

Bending Test

The bending characteristics and ultimate bending strength of UHPCs were confirmed by developing beam specimens made of UHPCs and conducting bending tests on them. An outline of the bending test is shown in Figure 2. Three specimens, one for each specimen of Fc150, UFC+Fc33, and Fc33, were tested. Referring to the criteria for APC with normal concrete, the loading on each specimen was applied with a ductility factor of approximately 10.

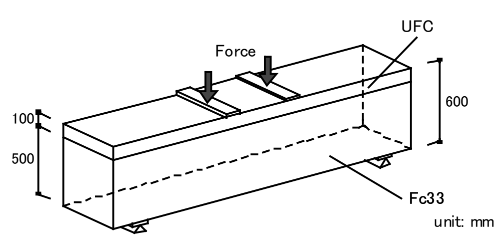

Figure 2. Outline of bending test (in the case of UFC+Fc33)

Figure 3 shows the cross sections of the specimens that describe the details of the specimens. As shown in Figure 3 (a), the Fc150 and Fc33 specimens were normal RC beams, which indicates that the specimens were reinforced by steel bars. On the other hand, because the specimen using UFC was a composite member with normal concrete Fc33, it had a cross section ratio of UFC: Fc33 = 1: 5, as shown in Figure 3 (b). To ensure integrity as one composite member, shear keys were shaped at the boundary between the two materials. The concrete strengths at the time of the tests are listed in Table 1. The reinforcement arrangements of the specimens are illustrated in Figure 4. The tension reinforcement ratio was set to p_t = 1.38%, referring to that of the general NPP buildings members.

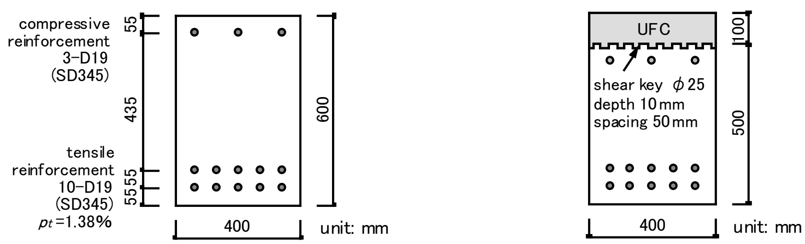

(a) Fc150 and Fc33 (b) UFC+Fc33

Figure 3. Cross sections of specimens

Table 1: Average of compressive strength at the time of loading test

Specimen		The average of compressive strength at the loading test (N/mm^2)
Fc150		162
UFC+Fc33	UFC	229
	Fc33	39.2
Fc33		37.6

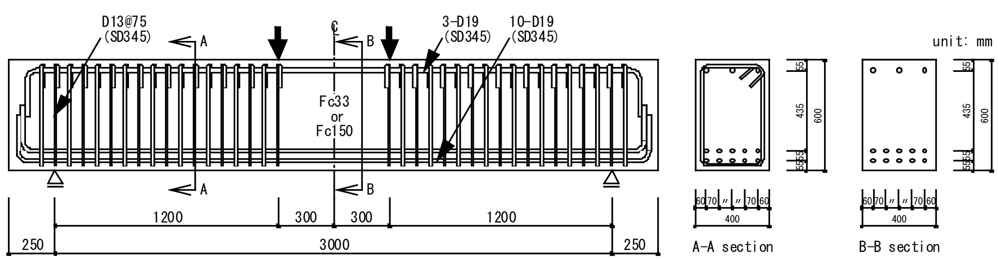

(a) Fc150, Fc33

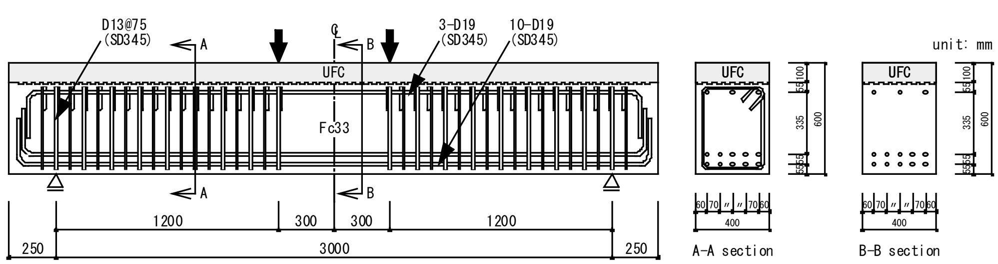

(b) UFC+Fc33

Figure 4. Reinforcement arrangement of specimens

During the test, the displacement and strain of the specimens were measured. However, the strain values around the end of the loading could not be obtained because the strain gauges broke owing to the cracks in the specimens. The strains in the extreme compression fiber of the specimens obtained by the strain gauges and those calculated from the displacement sensor based on the Navier hypothesis were confirmed to be almost the same until the strain gauges broke. Therefore, in this study, the compressive strains calculated from the displacement sensors were used as the experimental strains.

Photo 1 shows the states of the specimens at each deformation, and Figure 5 shows the load–displacement curves of the specimens. Because of the above-mentioned reason, the compressive strain values in each photo label are the values calculated at the center of the upper surface of the specimens based on the Navier hypothesis from the displacement sensors installed on the specimens. In the Fc33 specimen, the upper end of the beam was completely crushed at the end of the test; however, this was not observed in the Fc150 and UFC+Fc33 specimens, even at the end of the loading test. In the Fc150 specimen, the shear force did not decrease until the end of the test and the strain at the center of the upper surface was approximately 10,000 μ. In the UFC+Fc33 specimen, the shear force increased at the end of the test, and the strain was approximately 3400 μ, which was much smaller than those of the Fc150 and Fc33 specimens.

	$\delta = 20mm(\varepsilon_c = -2340\mu)$	$\delta = 35mm(\varepsilon_c = -3650\mu)$	$\delta = 60mm(\varepsilon_c = -6500\mu)$	$\delta = 85mm(\varepsilon_c = -10460\mu)$
Fc150	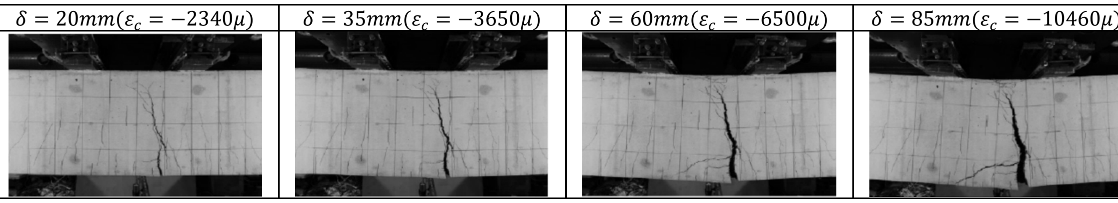			

	$\delta = 20mm(\varepsilon_c = -1710\mu)$	$\delta = 35mm(\varepsilon_c = -2140\mu)$	$\delta = 60mm(\varepsilon_c = -2460\mu)$	$\delta = 85mm(\varepsilon_c = -3420\mu)$
UFC +Fc33	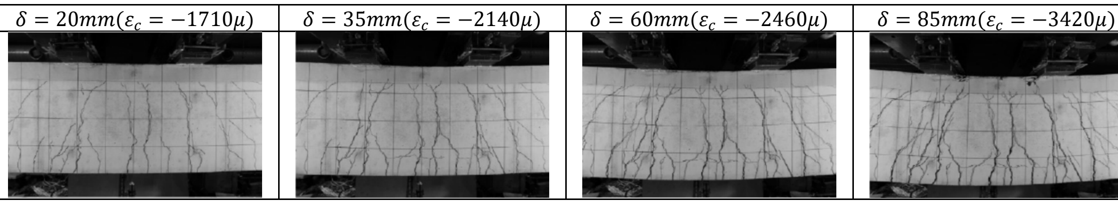			

	$\delta = 20mm(\varepsilon_c = -2620\mu)$	$\delta = 35mm(\varepsilon_c = -6500\mu)$	$\delta = 60mm(\varepsilon_c = -19240\mu)$	$\delta = 85mm(\varepsilon_c = -37410\mu)$
Fc33	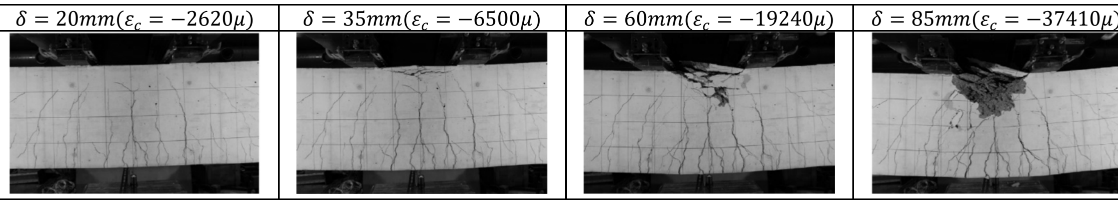			

Photo 1. States of specimens at each deformation

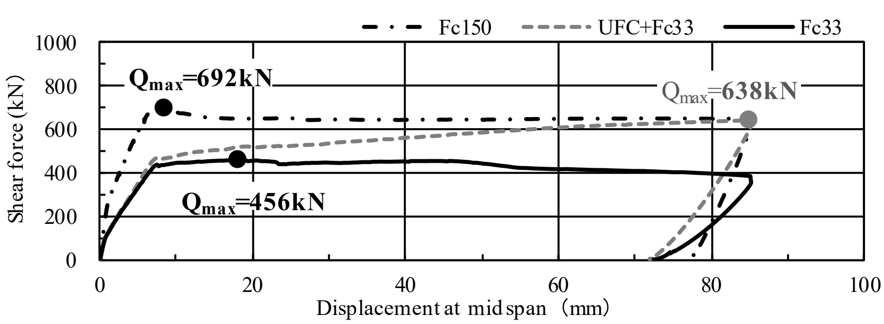

Figure 5. Load–displacement curves of specimens

Simulation Analysis of Bending Test

To confirm whether the behavior could be simulated analytically even when the UHPCs were contained, a finite element method (FEM) analysis of the specimens with UHPCs was conducted. The FEM software DIANA 10.2 was used. The analysis was performed using a two-dimensional model, and the concrete was modelled using shell elements and reinforcement bars with embedded bar elements. The FE models of specimens Fc150 and UFC+Fc33 are shown in Figures 6 and 7, respectively. Assuming the application of this simulation method to the actual assessment, the material physical values were set with the nominal values. However, in this study, to confirm whether the behavior of the concrete part can be simulated even with the nominal value, the physical values of the reinforcement were set to be the same as the experimental values. The set of physical values are listed in Tables 2 and 3.

Similarly, the constitutive models of FEM used in the general assessment in Japan were adopted because the purpose of this study is to establish an assessment method against global bending failure caused by APC. In Japan, a model without softening curve after compressive strength (constant stress–strain curve) was adopted as a constitutive model in concrete compression because of the convergence of the analysis. Therefore, the same model as that of the concrete compressive constitutive model was used in this study. For Fc33, the strain softening model in the Japan Society of Civil Engineers (JSCE, 2007) was adopted as concrete tensile constitutive model. For materials Fc150 and UFC+Fc33, a simplified strain softening model, which can simulate the result of the test piece experiment simultaneously performed with the bending test, was adopted. The adopted concrete constitutive models are shown in Figure 8. The reinforcement constitutive model is shown in Figure 9.

(a) Concrete (b) Reinforcement

Figure 6. FE model of Fc150 and Fc33 specimens

(a) Concrete (b) Reinforcement

Figure 7. FE model of UFC+Fc33 specimen

Table 2: Physical values of concrete

concrete		compressive strength fc(N/mm^2)	Young's modulus E(N/mm^2)	Poisson's ratio ν
Fc150		150	45,500	0.2
UFC+Fc33	UFC	180	52,300	0.2
	Fc33	33	25,200	0.2

Table 3: Physical values of reinforcement

reinforcement	yield strength ft(N/mm^2)	Young's modulus E(N/mm^2)	Poisson's ratio ν
SD345	384	189,000	0.3

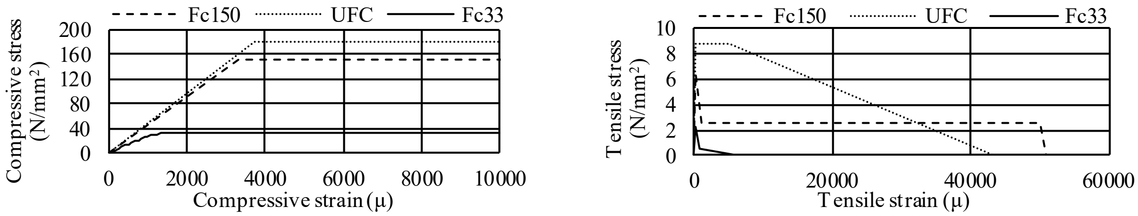

(a) Stress–strain curves of compression (b) Stress–strain curves of tension

Figure 8. Constitutive model of concrete

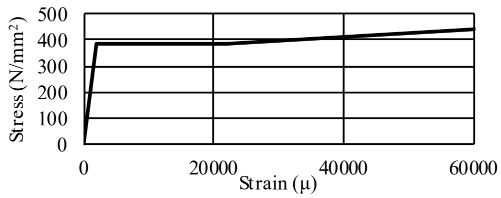

Figure 9. Constitutive model of reinforcement

Figure 10 shows the load–displacement curves of the experiment and analysis. It can be confirmed that the FEM analysis can simulate the load–displacement curves of both Fc150 and UFC+Fc33 specimens, and the strains of the simulation at the center of the upper surface are consistent with the results shown in Photo 1. Because the experimental results can be simulated in the analysis using the nominal values and the concrete constitutive model with constant stress after compressive strength, the analysis method in this study is applicable to assessments of actual plants. In addition, it is confirmed that the proof stress does not decrease and soundness is maintained until the strains of 10,000 and 5,000 μ for Fc150 and UFC+Fc33, respectively. Especially for the UFC+Fc33 specimen, the proof stress was gradually increasing even when the test was terminated at a displacement corresponding to the member ductility factor of 10. There is a possibility the proof stress can be maintained even at a larger strain.

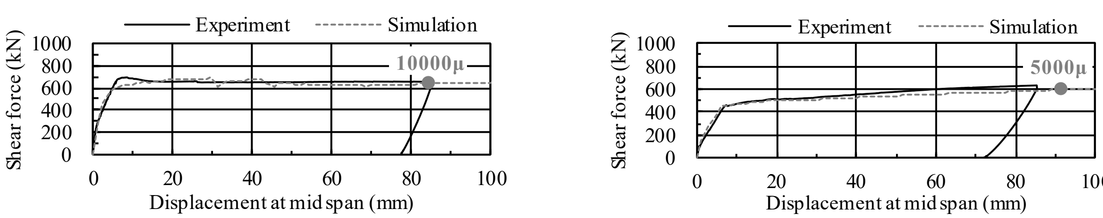

(a) Fc150 (b) UFC+Fc33

Figure 10. Load–displacement curves

STUDY OF PUNCHING SHEAR PERFORMANCE

Punching shear tests were conducted on the specimens with UHPCs to determine whether the existing evaluation formula for the ultimate punching shear strength is applicable to UHPCs.

Punching Shear Test

Similar to the bending tests, punching shear tests were conducted with Fc150, UFC+Fc33, and Fc33 specimens. An outline of the test setup is shown in Figure 11. Figure 12 shows the arrangement of the reinforcements. The specimens were square plates with a thickness, width, and tension reinforcement ratio of 120 mm, 1200 mm, and 0.49%, respectively, which are almost the same as those of specimens on the RC slabs of NPP buildings in the previous research. Photo 2 shows the cross sections of the specimens after the tests. The compressive strengths of the concrete at the time of the tests are listed in Table 4.

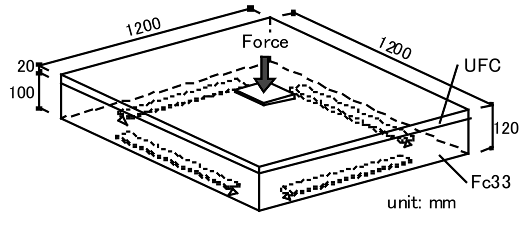

Figure 11. Outline of punching shear test (in the case of UFC+Fc33)

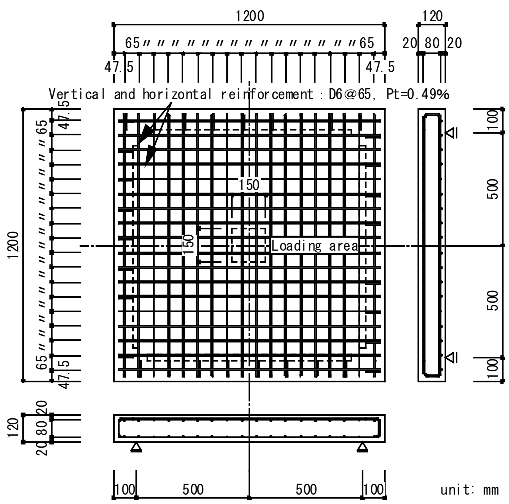

(a) Fc150 and Fc33

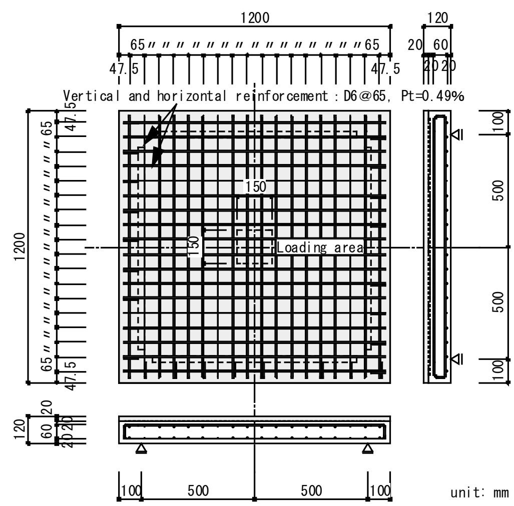

(b) UFC+Fc33

Figure 12. Arrangement of reinforcement

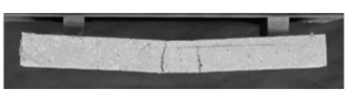

(a) Fc150

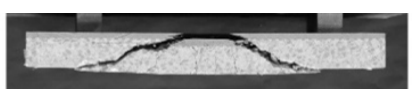

(b) UFC+Fc33

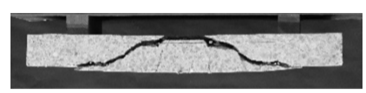

(c) Fc33

Photo 2. Cross section of specimens after test

Table 4: Average of compressive strength at the time of loading test

Specimen		The average of compressive strength at the loading test (N/mm^2)
Fc150		152
UFC+Fc33	UFC	226
	Fc33	37.6
Fc33		36.6

Evaluation of Ultimate Punching Shear Strength by Existing Formula

The design formula for UHPCs is shown in JSCE (2007). The formula in JSCE, as shown in Equation 1, calculates the punching shear capacity of the planar member (V_{pcd}) by multiplying the concrete strength (f_{pcd}), peripheral length of the evaluated cross section (u_p) shown in Figure 13 (a), effective height (d), and correction coefficients (β_d, β_p, and β_r). The JSCE formula has the upper limit of the concrete strength ($f_{pcd} \leq 1.2$ N/mm^2); however, to take advantage of the high concrete strength of UHPCs, the upper limit is ignored in the calculation. Moreover, the safety factor γ_b for design is 1.0 in this study (but it must be considered in actual design). In addition, this study proposes an evaluation method for composite member, as shown in Figure 13 (b). In other words, the total punching shear strength of the composite member was calculated by summing the punching shear capacity with the JSCE formula for each material.

$$V_{pcd} = \beta_d \cdot \beta_p \cdot \beta_r \cdot f_{pcd} \cdot u_p \cdot d \,/\, \gamma_b \tag{1}$$

where,

$f_{pcd} = 0.20\sqrt{f'_{cd}}$ (N/mm^2) (where $f_{pcd} \leq 1.2$N/mm^2; however since this study focuses on improving the punching shear strength by utilizing UHPCs, the upper limit is ignored here.)

$\beta_d = \sqrt[4]{1000/d}$ (d:mm) $\beta_d \leq 1.5$ (Coefficient of effective depth)

$\beta_p = \sqrt[3]{100p}$ $\beta_p \leq 1.5$ (Coefficient of reinforcement ratio)

$\beta_r = 1 + \dfrac{1}{\left(1 + 0.25\dfrac{u}{d}\right)}$ $1 \leq \beta_r \leq 2$ (Coefficient of the effect of loaded area)

f'_{cd}: compressive strength of concrete (N/mm^2)

u: peripheral length of loaded area

u_p: peripheral length of the design cross section located at a distance $d/2$ from the loaded area

d and p: effective depth and reinforcement ratio defined as the average values for the reinforcement in two directions.

γ_b: member factor. Generally, it may be taken as 1.3 (In this study, it was taken as 1.0).

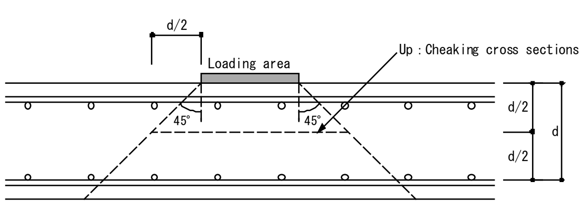

(a) Single material slab (Fc150 and Fc33)

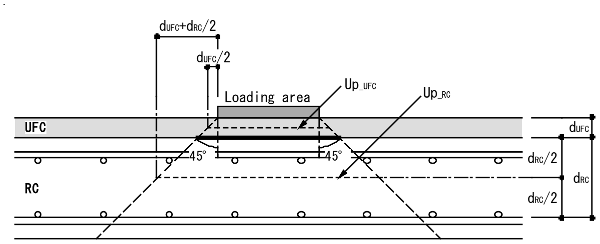

(b) Composite material slab (UFC+Fc33)

Figure 13. Loading area and peripheral length of cross section

The load–displacement curves and ultimate punching shear strengths of the tests are shown in Figure 14. The punching shear capacity of the specimens calculated using the above method is also shown in Figure 14. A comparison between the experimental and calculated values is presented in Table 5. Figure 15 shows the relationship between the experimental and calculated values of this study and those of the previous studies. They correspond well (because the results line up on the 45 °line in Figure 15); therefore, it is considered that the punching shear strength of the UHPCs can be evaluated using the JSCE formula.

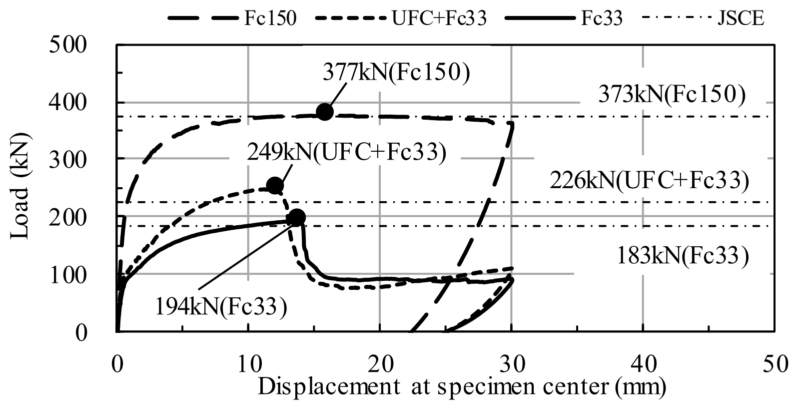

Figure 14. Load–displacement curves of specimen center

Table 5: Comparison of punching shear strength in experimental and calculated values

Specimen	Calculated value*1 (kN)	Experimental value (kN)	Experimental value / Calculated value
Fc150	373	377↑*2	1.01↑*2
UFC+Fc33	226	249	1.10
Fc33	183	194	1.06

*1: by JSCE formula
*2: Owing to the specimen fractured by bending, the ultimate punching shear strength was larger than this value.

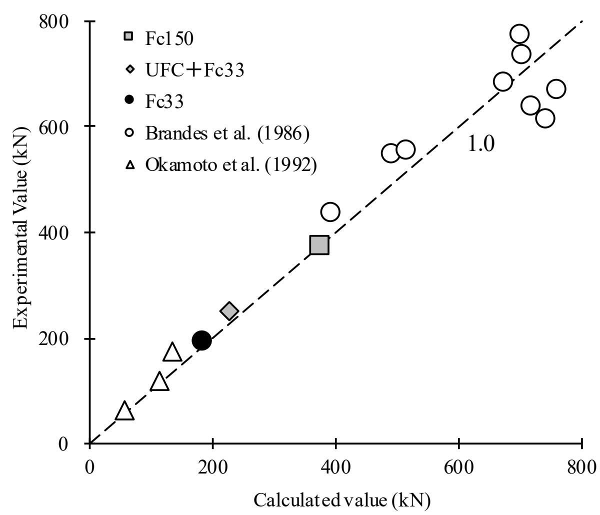

Figure 15. Relationship between experimental and calculated values of punching shear strength

CONCLUSION

In this study, the basic characteristics and ultimate resistance of ultra-high-performance-concretes (UHPCs) against impact loadings such as aircraft impact and tornado missiles to the walls and roofs of buildings in nuclear power plants (NPPs) were confirmed. Fc150 and UFC were selected as UHPCs. Fc150 is ultra-high-performance steel-fiber-reinforced concrete containing polypropylene fiber and UFC is ultra-high-performance steel-fiber-reinforced concrete. Fc150 contains coarse aggregate whereas UFC does not. The bending and punching shear tests were conducted to understand the basic characteristics of UHPCs related to global failure of walls etc. caused by impact loading. Using the bending test, it was confirmed that the members of UHPCs have superior deformation performance than that of normal concrete and that their behavior could be simulated using FEM analysis. Using the punching shear test, it was confirmed that the ultimate punching shear strength of the member with UHPCs could be evaluated using the existing JSCE formula. Understanding these basic characteristics, enables to conduct simulation studies in actual NPP buildings using UHPCs.

Because the number of specimens in this study was limited, conducting more tests is required in the future to expand our knowledge regarding the impact resistance of UHPCs.

ACKNOWLEDGEMENT

This study had been carried out in "the project on development of technical basis for improving nuclear safety" funded by Ministry of Economy, Trade and Industry (METI).

REFERENCES

Brandes, K., Limberger, E., Herter, J., and Berner, K. (1986). "Kinetic Load Bearing Capacity of Reinforced Concrete Members under Impact Load", *BAM,* Berlin, Germany, 131.

Japan Society of Civil Engineers. (2007). *Standard Specifications for Concrete Structures*. Shinjuku, Tokyo, Japan.

Nuclear Energy Institution. (2011). *Methodology for Performing Aircraft Impact Assessments for New Plant Designs*, Washington, DC, USA, 07-13.

Okamoto, S., Imamura, A., Kasai, Y., and Ono, H. (1992). "Study on the Deformation and Failure Modes of Reinforced Concrete Slab Subject to a High-Speed Load. Part 2 result of the testing.," *Summaries of technical papers of annual meeting*, Architectural Institute of Japan, Minato, Tokyo, Japan, 323-324. (in Japanese)